

Analysis of Activation-Recovery Intervals from Intra-cardiac Electrograms in a Pre-clinical Chronic Model of Myocardial Infarction

Danielle Denisko¹, Samuel Oduneye^{1,2}, Philippa Krahn^{1,2}, Sudip Ghate²,
Ilan Lashevsky³, Graham Wright^{1,2}, and Mihaela Pop^{1,2}✉

¹ Department of Medical Biophysics, University of Toronto, Toronto, Canada
mihaela.pop@utoronto.ca

² Sunnybrook Research Institute, Toronto, Canada

³ Arrhythmia Services Sunnybrook, Toronto, Canada

Abstract. Mapping of intracardiac electrical signals is a well-established clinical method used to identify the foci of abnormal heart rhythms associated with chronic myocardial infarct (a major cause of death). These foci reside in the ‘border zone’ (BZ) between healthy tissue and dense collagenous scar, and are the targets of ablation therapy. In this work we analyzed detailed features of the electrical signals recorded in a translational animal model of chronic infarct. Specifically, activation maps and bipolar voltages were recorded in vivo from 6 pigs at ~5 weeks following infarct creation, as well as 6 control (normal) pigs. Endocardial and epicardial maps were obtained during normal sinus rhythm and/or pacing conditions via X-ray guided catheter-based mapping using an electro-anatomical CARTO system. The depolarization and repolarization maps were derived through manual annotation of electro-cardiogram waves, where the peak of the QRS wave marked the time of depolarization and the peak of the T wave marked the recovery time. Then, at each recording point, activation-recovery intervals ARIs (clinical surrogates of action potential duration) were found by subtracting activation times from repolarization times. Overall, we observed that ARI values in the BZ have recovered from the acute stage and were close to values in healthy tissue. In general we observed a weak negative correlation between the activation times and ARI values, also not a significant variation ($p < 0.5$) between mean ARI values in the BZ area and those in the healthy areas.

Keywords: CARTO electro-anatomical mapping · Bipolar voltages · Chronic infarct · Fibrosis · Border zone · Activation-recovery intervals

1 Introduction

Abnormal propagation of the electrical impulse in patients with prior myocardial infarction is a major cause of sudden cardiac death (SCD) in the industrialized world [1]. Structurally, a chronic infarct is comprised of a dense scar (collagenous fibrosis) and a border zone, BZ (also known as the peri-infarct). The latter is a ‘heterogeneous’ tissue, being comprised of a mixture of viable myocytes and collagen fibers [2]. Electrically,

the scar is non-conductive, whereas the BZ has reduced tissue conductivity (i.e., the action potential wave propagates slower than in the normal myocardium) [3]. These structural and electrical heterogeneities can trigger lethal ventricular arrhythmias such as ventricular tachycardia (VT), and ventricular fibrillation (VF) [4]. Thus, an important clinical task is the evaluation of disease severity and localization of BZ (the substrate of VT/VF) in patients with scar-related arrhythmia, along with the assessment of changes in tissue structure and electrical properties during infarct healing.

In the clinical laboratory, non-invasive imaging methods and various (more or less minimally) invasive electrophysiology (EP) tools have been intensively employed in the past decade. To date, several groups have demonstrated that the VT foci reside in the ‘border zone’ (BZ) between healthy tissue and collagenous scar, and can be structurally identified using MR imaging [5, 6]. Other studies have shown that infarct and BZ regions identified in *ex vivo* and *in vivo* MR images correlated well the location of these areas identified in electrical maps (by optical fluorescence imaging or unipolar/bipolar voltage maps) [7–9]. These studies provided a better tissue characterization in the dense scar and BZ, the latter being the target of a potential curative therapy known as RF thermal ablation [10]. However, there is a lack of thorough characterization of electrical signals in these critical tissue areas, and for this reason conventional unipolar/bipolar EP mapping often fails to localize the BZ in the clinical EP lab [11]. Furthermore, the action potential wave cannot be recorded directly *in vivo* via conventional EP catheters; thus, other methods are sought to identify such electrical characteristics of BZ.

The purpose of this work was to better understand the subtle characteristics of electrical signals in the peri-infarct, using a reproducible pre-clinical animal model of chronic infarction that mimics the post-infarct pathophysiology in humans. Specifically, here we focused on analyzing the features of intra-cardiac electrical signals in the BZ area by studying the *activation-recovery interval* (ARI), a clinical surrogate of action potential duration, APD [12]. We hypothesized that ARIs derived from locally-recorded activation maps (i.e., depolarization and repolarization times) can help identify distinctive diagnostic features in the BZ.

2 Materials and Methods

All *in vivo* experiments included in this study received ethics approval by our research institute. In this work, we performed X-ray guided electro-anatomical mapping studies in a swine model. This particular animal model is advantageous to use in translational frameworks, because the heart size and the infarct pathophysiology are close to those of human heart. Specifically, we performed catheter-based EP mapping experiments in 6 normal and 6 chronically infarcted swine, followed by data analysis to characterize ARIs in healthy tissue, dense scar and BZ.

2.1 Animal Model of Infarction

Myocardial infarction was created in juvenile swine (~30 kg) under X-ray guidance via a balloon catheter (Fig. 1). This catheter (indicated by the white arrow) was inserted and

inflated into a major coronary artery (e.g. either the left anterior descendant LAD or the left circumflex artery, LCX), using a 90 min occlusion-reperfusion method. The lesions were then allowed to heal for ~5 weeks as in our previous studies [13]. At this time point post-infarction, edema had resorbed and the core of the chronic lesion is replaced by mature collagen (evident in the Masson Trichrome stain), while the BZ was characterized by a patchy fibrosis, with altered electrical properties as observed in Fig. 1 from the decreased density in gap junctions, Cx43 (in agreement with [14]). The Cx43 protein is responsible for the cell-to-cell electrical conduction through the flow of ionic current [15]; its inhibition results in a slower conduction of the electrical impulse and triggers VT.

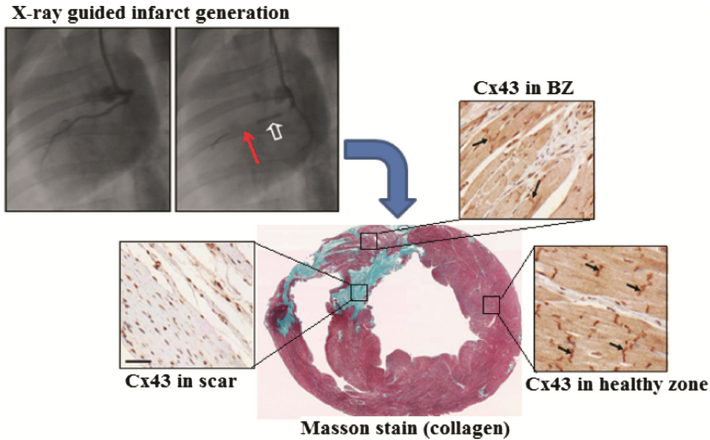


Fig. 1. X-ray guided infarct creation in a swine model (red arrow indicates the cessation of flow during the 90 min occlusion of LAD), along with histological images demonstrating deposition of dense fibrosis in the scar, a mixture of viable and collagen in BZ, and a decreased density in gap junctions (Cx43) in BZ. (Color figure online)

2.2 *In Vivo* Electro-Anatomical Mapping Study and ARI Analysis

Intra-cardiac waves, along with unipolar and bipolar voltage maps, were recorded by a catheter-based invasive method using a contact electro-anatomical mapping system (i.e., CARTO-XP, Biosense, USA). Some maps were recorded from the left ventricle (LV) endocardium and others from the epicardium, and some from both the LV-endo and epicardium. The electrical signals were acquired under sinus rhythm or pacing conditions (via a secondary catheter inserted at the apex of right ventricle, RV) from normal and infarcted pigs. During acquisition, cut-off filters were applied to measure only the signals within 30–400 Hz.

Figure 2 shows typical surfacic voltage maps recorded via a QuickStar catheter (2a) from the endocardial LV of an infarcted swine (2b) and a normal swine (2c), along with examples of intracardiac ecg-s waves from healthy tissue (pink), dense scar (red) and BZ (blue/green). These categories were defined based on clinical accepted thresholds: healthy tissue >1.5 mV; dense scar <0.5 mV; and, 0.5 mV $<$ BZ $<$ 1.5 mV [16].

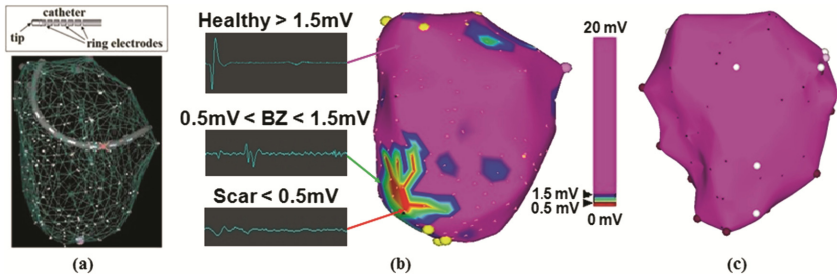


Fig. 2. Example of catheter-based electrical recordings from infarcted and normal pigs. (Color figure online)

For analysis, the activation-recovery intervals (ARIs) were determined for all intra-cardiac unipolar waves using the Wyatt method using the QRS and T waves [12]. Briefly, for each intra-cardiac wave, a local repolarization time (LRT) was found for biphasic and negative deflections using dV/dt_{max} (maximum rate of rise of voltage), whereas for positive deflections we used dV/dt_{min} on the descending limb of the T-wave. Finally, ARI was calculated as the difference between LRT and LAT (Fig. 3), as per the method proposed in [17]. All calculations and annotations were manually performed off-line using the CARTO analysis software.

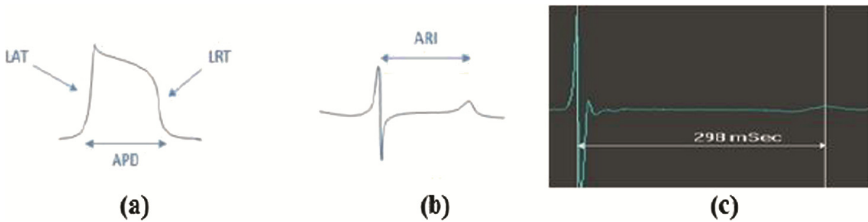


Fig. 3. Relation between (a) APD vs (b) ARI; and (c) an annotated sample of intracardiac ecg signal from a healthy myocardial tissue.

3 Results

Figure 4 shows an example of endocardial activation maps from the LV of a normal pig during normal sinus rhythm, NSR. Note that the earliest time point is in red and the latest activation time is depicted in purple. The propagation of depolarization wave starts in the anterior mid-septum and ends close to the mitral valve (see depolarization map in Fig. 4a). The repolarization follows a similar sequence (see repolarization map in Fig. 4b). The ARI map shows an opposite sequence, with shortest values near mitral valve, and longest near the septum (as clearly depicted in Fig. 4c).

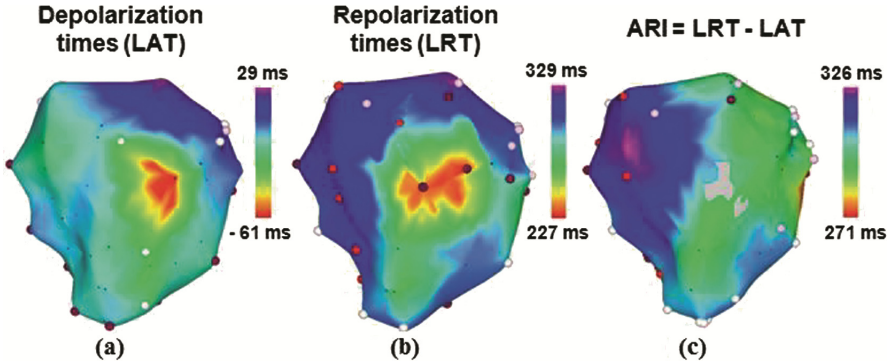


Fig. 4. Endocardial activation times reconstructed from CARTO recordings in the LV of a normal pig: (a) depolarization map (LAT); (b) repolarization (LRT) map; and (c) ARI map.

Figure 5 shows an example of endocardial LV maps from an infarcted heart, obtained under paced conditions (i.e., pacing catheter placed at the apex of RV). The earliest activation in the depolarization (LAT) map at site of the action potential wave break-through the septum, is in red. Notable here is a dispersion of repolarization near the dense scar region as evident in the associated LRT map. In this case, the repolarization sequence is opposite to the activation sequence (as compared to the normal case described in Fig. 4). The spatial pattern of the ARI closely follows the LRT pattern.

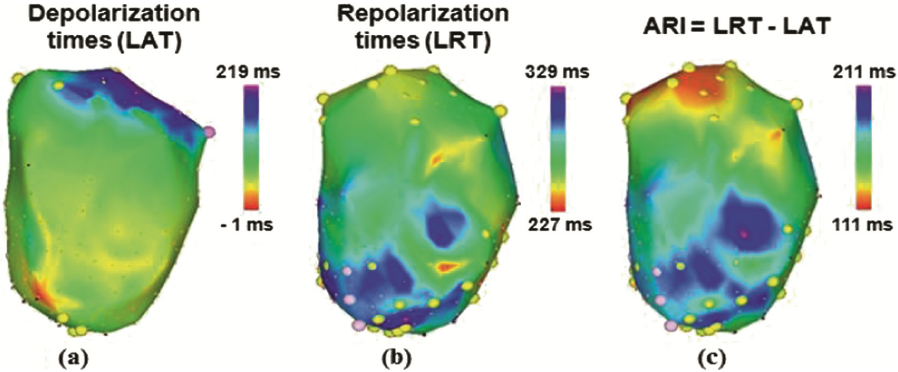


Fig. 5. Endocardial activation times reconstructed from CARTO recordings in the LV of an infarcted pig (note: the LAT map was recorded during pacing from RV): (a) depolarization map; (b) repolarization map; and (c) ARI map.

Figure 6 shows quantitative results of ARI calculations as a function of depolarization time recorded in LV. Notable is the clear separation of NSR data vs paced data, where the pacing cycle length (CL) was 400 ms in the LV of a normal heart (Fig. 6a). In contrast, we observed a significant overlap of the data points in the infarcted hearts in both healthy tissue areas (Fig. 6b) and BZ area (Fig. 6c), where the pacing CL was ~550–600 ms.

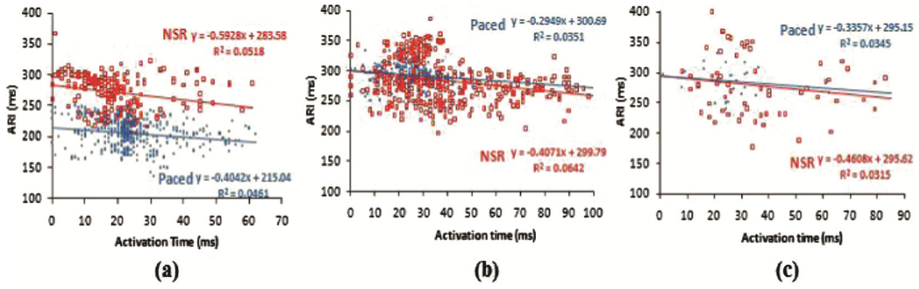


Fig. 6. Plots of ARI as a function of depolarization times (see text for details)

The number of recording points in the CARTO maps varied between 65 to ~200 points (with the less dense maps corresponding to the normal hearts).

Figure 7 shows a comparison between the mean ARI recorded in NSR from the LV-endo vs. epicardium of normal pigs and infarcted pigs (both areas: healthy and BZ). In the infarcted pigs, we obtained significant differences between the mean ARI in LV-endo and in epicardium, in the recordings from both healthy (remote) tissue ($p = 0.020$) and BZ ($p = 0.024$) tissue. Lastly, the differences in mean ARI between LV-endo and epicardium of normal pigs was found not significant ($p = 0.055$). Statistically significant differences were defined by p values < 0.05 and were calculated using [18].

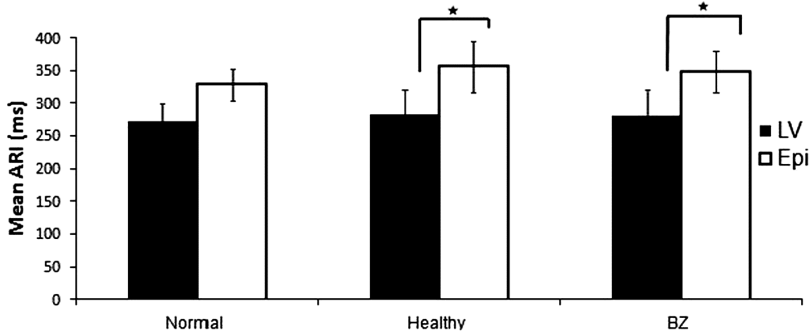


Fig. 7. Comparison between mean ARI in LV-endo vs. mean ARI in epicardium from different zones in normal and infarcted pigs (note: all recordings in NSR). At least 3 datasets were included in each category for averaging and statistical analysis. The error bars represent standard deviation (SD) (* $p < 0.05$).

4 Discussion

Accurate structural and electrical characterization of myocardial tissue in post-infarction remodelling is an important task in order to identify potential arrhythmogenic foci. Previous electrophysiology studies carried out in preclinical porcine models demonstrated that the amplitude of unipolar/bipolar waves can help detect the infarct location in electro-anatomical maps [19, 20]; however, these studies lacked the analysis of

intracardiac ecgs in the BZ. To the best of our knowledge, this study is the first to analyze in detail the ARIs (as an APD surrogate) in a pre-clinical model of chronic infarction.

Our mean ARIs and activation time ranges obtained in the normal porcine hearts (controls) agreed well with the only other existing study in normal pigs [17]. We also observed that mean ARI values in the BZ have recovered from the acute stage of infarction and were somewhat close to ARI values in normal tissue. This can be somewhat explained by a recovery of APD in the BZ about one month following infarction, as previously suggested by other studies [3]. Interestingly however, although the mean ARI values averaged over all pigs were not significant ($p < 0.5$), the ARI values were different between BZ and healthy areas per each animal (up to ~ 40 ms). This result suggests that, to ensure accurate predictions, the parameterization of computer models from ARI maps (an important step in our future work) should be performed on an individual heart basis rather than using mean values or literature values.

The negative correlation between ARI vs activation time, suggests coupling between both variables, which leads to a more simultaneous repolarization process. The AP wave exhibited a time delay between LV and RV propagation, and from endocardium to epicardium breakthrough. The effects of pacing followed the typical APD restitution curve, with an ARI shortening in response to faster pacing (although we acknowledge that the pacing was performed only at CLs of 400 ms, 550 ms and 600 ms). Shorter pacing CL (Fig. 7a) resulted in lower ARI while pacing at a CL similar to NSR CL had little effect (Fig. 7b, c). Another limitation of this study is the relatively small sample size included in each statistical analysis (i.e., the number of datasets included in each category: pacing vs. NSR, LV vs. epicardial mapping, etc.).

5 Conclusion

To sum up, we successfully developed a preclinical framework to analyze the features of electrical signals in an animal model of chronic infarction. We acknowledge that the current data was limited to intracardiac ecg recordings in either sinus rhythm, or at one pacing frequency, or both sinus and (per animal). Thus, our next steps will focus on performing more controlled pre-clinical experiments, with a particular focus on obtaining more pacing frequencies data in the same subject (e.g. 4–5 pacing frequencies besides the sinus rhythm), to enable a thorough analysis of the ARI characteristics during pacing. This will also allow us to perform a parameter fitting for restitution curves. Furthermore, we will focus on personalizing 3D MRI-based computer models per individual heart from *in vivo* electrical maps, enabling more accurate predictions of cardiac wave propagation and simulation of scar-related arrhythmia.

Acknowledgement. This work was financially supported in part by a grant from CIHR (MOP # 93531) and a summer student award D&H (Sunnybrook).

References

1. Stevenson, W.G.: Ventricular scars and VT tachycardia. *Trans. Am. Clin. Assoc.* **120**, 403–412 (2009)
2. Bolick, D., Hackel, D., Reimer, K., Ideker, R.: Quantitative analysis of myocardial infarct structure in patients with ventricular tachycardia. *Circulation* **74**(6), 1266 (1986)
3. Ursell, P.C., Gardner, P.I., Albala, A., Fenoglio, J., Wit, A.L.: Structural and electrophysiological changes in the epicardial border zone of canine myocardial infarcts during infarct healing. *Circ. Res.* **56**, 436–451 (1985)
4. Janse, M.J., Wit, A.L.: Electrophysiological mechanisms of ventricular arrhythmias resulting from myocardial ischemia and infarction. *Physiol. Rev.* **69**(4), 1049–1169 (1989)
5. Bello, D., Fieno, D.S., Kim, R.J., et al.: Infarct morphology identifies patients with substrate for sustained ventricular tachycardia. *J. Am. Coll. Cardiol.* **45**(7), 1104–1110 (2005)
6. Pop, M., Ghugre, N.R., Ramanan, V., Morikawa, L., Stanisz, G., Dick, A.J., Wright, G.A.: Quantification of fibrosis in infarcted swine hearts by ex vivo late gadolinium-enhancement and diffusion-weighted MRI methods. *Phys. Med. Biol.* **58**(15), 5009 (2013)
7. Yan, A., Shayne, A., Brown, K., Gupta, S., Chan, C., Luu, T., Di Carli, M., Reynolds, H., Stevenson, W., Kwong, R.: Characterization of the peri-infarct zone by contrast-enhanced cardiac magnetic resonance imaging is a powerful predictor of post-myocardial infarction mortality. *Circulation* **114**, 32 (2006)
8. Wijnmaalen, A., van der Geest, R., van Siebelink, C.F.B.H., Wijnmaalen, H., Kroft, L., Bax, J., Reiber, J., Schalij, M., Zeppenfeld, K.: Head-to-head comparison of contrast-enhanced magnetic resonance imaging and electroanatomical voltage mapping to assess post-infarct scar characteristics in patients with ventricular tachycardias: real-time image integration and reversed registration. *Eur. Heart J.* **32**, 104 (2011)
9. Pop, M., Sermesant, M., Liu, G., Relan, J., Mansi, T., Soong, A., Peyrat, J.-M., Truong, M.V., Fefer, P., McVeigh, E.R., Delingette, H., Dick, A.J., Ayache, N., Wright, G.A.: Construction of 3D MR image-based computer models of pathologic hearts, augmented with histology and optical imaging to characterize the action potential propagation. *Med. Image Anal.* **16**(2), 505–523 (2012)
10. Verma, A., Kilicaslan, F., Schweikert, R., Tomassoni, G., Rossillo, A., Marrouche, N., Ozduran, V., Wazni, O., Elayi, S., Saenz, L., et al.: Short-and long-term success of substrate-based mapping and ablation of ventricular tachycardia in arrhythmogenic right ventricular dysplasia. *Circulation* **111**(24), 3209 (2005)
11. Desjardins, B., Crawford, T., Good, E., Oral, H., Chugh, A., Pelosi, F., Morady, F., Bogun, F.: Infarct architecture and characteristics on delayed enhanced MR imaging and electroanatomic mapping in patients with postinfarction ventricular arrhythmia. *Heart Rhythm* **6**(5), 644–651 (2009)
12. Haws, C.W., Lux, R.L.: Correlation between in vivo transmembrane APD and ARI from EGM. *Circulation* **81**(1), 281–288 (1989)
13. Pop, M., Ramanan, V., Yang, F., Zhang, L., Newbigging, S., Ghugre, N., Wright, G.A.: High resolution 3D T1* mapping and quantitative image analysis of the gray zone in chronic fibrosis. *IEEE Trans. Biomed. Eng.* **61**(12), 2930–2938 (2014)
14. Zhang, Y., Wang, H., Kovacs, A., Kanter, E.M., Yamada, K.A.: Reduced expression of Cx43 attenuates ventricular remodelling after myocardial infarction via impaired TGF- β signaling. *Am. J. Physiol. Heart Circ. Physiol.* **298**(2), H477–H487 (2010)
15. Jansen, J., van Veen, T.A.B., de Jong, S., van der Nagel, R., van Rijen, H.V.M., et al.: Reduced Cx43 expression triggers increased fibrosis due to enhanced fibroblast activity. *Circ. Arrhythmia Electrophysiol.* **5**, 380–390 (2012)

16. Codreanu, A., Odille, F., Aliot, E., et al.: Electro-anatomic characterization of post-infarct scars comparison with 3D myocardial scar reconstruction based on MR imaging. *J. Am. Coll. Cardiol.* **52**, 839–842 (2008)
17. Gepstein, L., Hayam, G., Ben-Haim, S.A.: Activation-repolarization coupling in the normal swine endocardium. *Circulation* **96**, 4036–4043 (1997)
18. www.vassarstats.net
19. Wroblewski, D., Houghtaling, C., Josephson, M.E., Ruskin, J., Reddy, V.: Use of electrogram characteristics during sinus rhythm to delineate the endocardial scar in a porcine model of healed myocardial infarction. *J. Cardiovasc. Electrophysiol.* **14**, 524–529 (2003)
20. Callans, J.D., Ren, J.-F., Michele, J., Marchlinski, F., Dillon, S.: Electroanatomic left ventricular mapping in the porcine model of healed anterior myocardial infarction. Correlation with intracardiac echocardiography and pathological analysis. *Circulation* **100**, 1744–1750 (1999)